Printing-based performance analysis of the engineering test stand set-2 optic using a synchrotron exposure station with variable sigma

Patrick Naulleau,[a] Kenneth A. Goldberg, and Erik H. Anderson
Center for X-Ray Optics, Lawrence Berkeley National Laboratory, Berkeley, California 94720

Jeffrey Bokor
Center for X-Ray Optics, Lawrence Berkeley National Laboratory and EECS Department, University of California, Berkeley, California 94720

Bruce Harteneck, Keith Jackson, Deirdre Olynick, and Farhad Salmassi
Center for X-Ray Optics, Lawrence Berkeley National Laboratory, Berkeley, California 94720

Sherry Baker, Paul Mirkarimi, Eberhard Spiller, and Chris Walton
Lawrence Livermore National Laboratory, P.O. Box 808, Livermore, California 94550

Donna O'Connell
Sandia National Laboratories, P.O. Box 969, Livermore, California 94551

Pei-Yang Yan and Guojing Zhang
Intel Corporation, 2200 Mission College Boulevard, Santa Clara, California 95052

(Received 2 July 2003; accepted 2 September 2003; published 5 December 2003)

While interferometry is routinely used for the characterization and alignment of lithographic optics, the ultimate measure of performance for these optical systems is the transfer of an image or pattern into photoresist. Simple yet flexible exposure systems play an important role in this task because they allow complex system-dependent effects to be isolated from the printing results. One such tool has been implemented for alpha-class extreme ultraviolet (EUV) optics at Lawrence Berkeley National Laboratory using a synchrotron-based illumination source with programmable coherence. This static microfield exposure system has been used to characterize a four-mirror optical system designed for the EUV engineering test stand prototype stepper. Here we present a detailed performance analysis based on the large volume of lithographic data collected from this 0.1 NA system. Process window results are presented for dark field and bright field nested features down to a half pitch of 70 nm (k_1 factor of 0.52) where a depth of focus of approximately 1 μm with 10% exposure latitude is demonstrated. [DOI: 10.1116/1.1621669]

I. INTRODUCTION

The push by the microelectronics industry to ever-smaller feature sizes will eventually force lithography used in high-volume manufacturing to deviate from the refractive optical system paradigm. This has led to the development of a variety of next-generation lithography techniques, of which extreme ultraviolet (EUV) projection lithography is now the leading contender.[1,2] While at-wavelength characterization[3–5] plays a crucial role in the development of EUV lithographic optics, the ultimate measure of lithographic quality is pattern transfer into photoresist. To address this concern, an alpha-class stepper [the EUV engineering test stand (ETS)] has been developed and is now operational at the Virtual National Laboratory (a collaboration among Lawrence Berkeley, Lawrence Livermore, and Sandia National Laboratories). Although ideal for the characterization of system-level issues, the complexity of such alpha tools limit their ability to systematically isolate the optical performance of the projection system from other system parameters such as illumination effects. In part for this reason, microfield static exposure tools[6–8] have played and are expected to continue to play a crucial role in the development and commercialization of EUV lithography.

One such tool is a static microfield printing system implemented at Lawrence Berkeley National Laboratory's Advanced Light Source synchrotron radiation facility.[8] Although not under serious consideration for manufacturing applications, synchrotron radiation provides a convenient well-characterized debris-free source for such microfield systems. While synchrotron sources are well suited to metrology applications,[3] the problem with using these sources for lithography is the poor match between the intrinsic coherence properties of the source and those required of a lithographic tool. Synchrotron radiation, with its inherently narrow divergence, is typically much more coherent than one desires for lithographic printing. To overcome this issue, an active custom-coherence scanning illuminator has been developed.[9] This system supports variable partial coherence (σ) ranging from approximately 0 to 1 and enables the generation of arbitrary pupil fills such as dipole and the ETS six-channel fill. Moreover, because the pupil fill is synthesized through a scanning process, as opposed to using fixed apertures, modifying the pupil fill is achieved without loss of optical throughput.

[a]Author to whom correspondence should be addressed; electronic mail: pnaulleau@lbl.gov

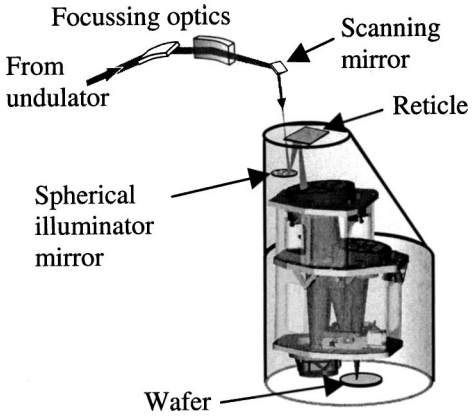

FIG. 1. Schematic of the Berkeley microfield exposure station.

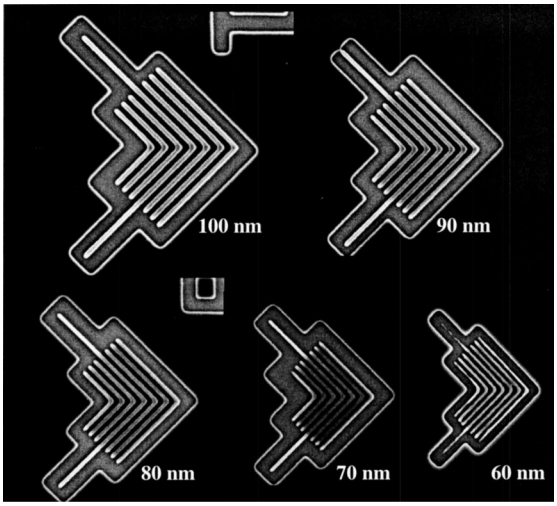

FIG. 2. Series of equal-line space elbow pattern images ranging from a half pitch of 100 down to 60 nm. The features were printed using a dark field mask where each elbow pattern is positioned in a local bright field slightly larger than the elbow pattern itself. The resist images were recorded in Shipley EUV-2D resist under conventional disk illumination with $\sigma=0.8$.

As previously described[8,10] the Berkeley exposure system has been used to lithographical characterize the second of two EUV 4× reduction optical systems[11] developed as part of the EUV Limited Liability Company's (LLC's) EUV lithography program. The first optic[5] was a developmental set dedicated to system integration learning in the ETS, whereas the second much higher quality optic[12] is intended for EUV lithographic learning. Although the Set-2 optic is now integrated into the ETS,[13] during its characterization at Berkeley, a wide variety of lithographic parameters were studied including, among others, illumination conditions, resist thickness, and mask tone. Here we present a subset of this data in terms of process-window results.

II. SYSTEM CONFIGURATION

The Berkeley exposure system (Fig. 1) has a static microfield size of approximately 100 μm at the wafer and works with the same reflection masks used in the ETS. Although the instantaneous static field size is small, the full 1 in. arc-shaped field of view can be covered one subfield at a time by moving the entire system (with the exception of the illuminator components) under the beam. The reticle stage, optic, and wafer stage are integrated into a single rigid structure that can be moved as a unit using a precise planar-bearing stage.

For optimal compatibility with the wave front interferometer[5] into which the printing system was integrated, the same high-resolution, small travel, stages are used in the two configurations. The drawback of this is that the total stage travel is limited to approximately 2 mm. However, due to the small 100 μm field size, as constrained by the illuminator design, focus-exposure matrices with up to approximately 20 elements in one direction can be achieved. The focus resolution of the wafer stage is approximately 100 nm, which is adequate for the 0.1 numerical aperture (NA) optic of concern here. The dose is adjusted by controlling the power output of the beamline while keeping the exposure time fixed as is required by the scanning illuminator.[9] Using this method, experimental results demonstrate a dose control capability of approximately 2%.

III. LITHOGRAPHIC EVALUATION OF THE ETS SET-2 OPTIC

As described above, the Berkeley static exposure system has been used to characterize ETS set-2 optic, a 0.1 NA optic operating at a wavelength of 13.4 nm. At the central field point, where the majority of the subsequent printing results were collected, the optic was interferometrically measured to have a 37 Zernike rms wave front quality of 0.69 nm or 52 mwaves with the dominant terms being spherical aberration and trifoil.[12] Based on this wave front quality, one expects near diffraction-limited performance. The Raleigh criterion (Res.$=0.61\lambda$/NA) predicts a resolution limit of approximately 82 nm.

Figure 2 shows a series of equal-line-space elbow pattern images ranging from a half pitch of 100 nm down to 60 nm. The features were printed using a dark field mask where each elbow pattern is positioned in a local bright field slightly larger than the elbow pattern itself. The resist images shown in Fig. 2 were all recorded in Shipley EUV-2D resist under conventional disk illumination with a σ of 0.8. Because the ETS set-2 optic has a NA of 0.1, these prints correspond to k_1 factors of 0.75–0.45, where $k_1=(\mathrm{CD})(\mathrm{NA})/\lambda$, where CD is the critical dimension. We note that utilizing dipole illumination the set-2 optic has been demonstrated to print 50 nm half pitch features ($k_1=0.375$) in one dimension.[8] Extrapolating these results to an EUV optic with 0.25 NA (the expected NA of the first EUV Beta tools), 40 nm CD would correspond to a k_1 factor of 0.75, equivalent to the 100 nm CD prints presented here. Moreover, achieving a k_1 factor of 0.52 (as was readily achieved here with conventional illumination) with an NA of 0.25 would result in 28 nm half-pitch printing.

As evidenced in Fig. 2, the printing process tends to break down, especially in terms of the iso-dense bias, at the 60 nm level. Modeling shows that although the optic itself is the

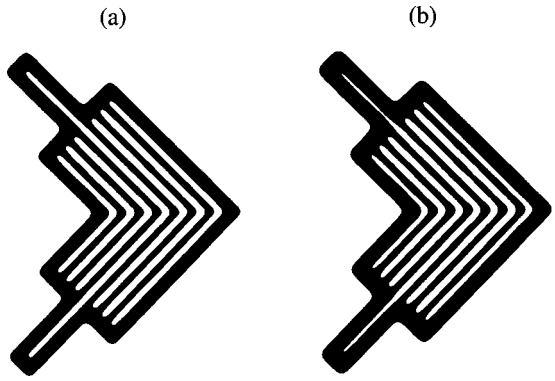

FIG. 3. Modeling results on 60 nm elbows showing that a majority of the image degradation effect can be attributed to resist limits. Using the full EUV-measured wave front incorporating the effects of flare to calculate the aerial image and assuming an ideal binary resist, results in the image shown in (a). Incorporating the effect of the resist yields the results shown in (b), qualitatively matching the experimental behavior seen in Fig. 2.

cause of some of the degradation, a majority of the effect can be attributed to resist limits. Using the full EUV-measured wave front, which incorporates the effects of flare over relevant dimensions, the aerial image of the 60 nm elbow pattern can be calculated [Fig. 3(a)]. The image in Fig. 3(a) is based on an ideal binary resist model. It is evident that aerial-image simulation does not predict the iso-dense bias. We note that the scalar model is sufficient for image calculation due to the small NA. Incorporating the effect of the resist as a simple 50 nm full-width-half-maximum (FWHM) Gaussian point-spread function (PSF), however, yields the results shown in Fig. 3(b), qualitatively matching the experimental behavior seen in Fig. 2. We note that modeling the effect of Shipley EUV-2D resist as a 50 nm FWHM Gaussian PSF is consistent with earlier contrast studies performed using two separate EUV optics and exposure systems.[14]

Although Fig. 2 demonstrates resolution down to approximately 60 nm half pitch, in practice, achievable resolution must be based on process-window size, or depth of focus (DOF) at a given exposure latitude (EL). The process-window results presented here correspond to $\pm 10\%$ CD change and the DOF is quoted with 10% EL. Figure 4 shows

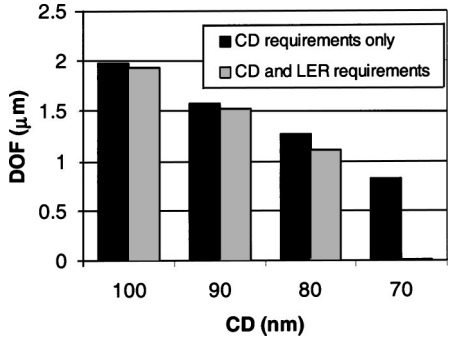

FIG. 4. DOF for nested dark field features down to 70 nm half pitch. The DOF is based on the $\pm 10\%$ CD change process window and an exposure latitude of 10%. Also shown is the line-edge roughness limited DOF based on a 3σ single-sided LER threshold of 10% of the nominal CD.

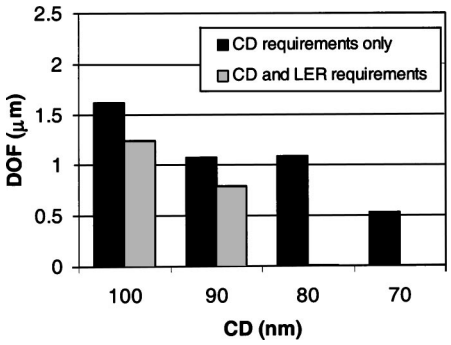

FIG. 5. DOF for nested bright field features down to 70 nm half pitch. The DOF is based on the $\pm 10\%$ CD change process window and an exposure latitude of 10%. Also shown is the line-edge roughness limited DOF based on a 3σ single-sided LER threshold of 10% of the nominal CD.

the DOF for nested dark field features down to 70 nm half pitch. The 60 nm case is not shown as no measurable process window was found. At 100 nm CD, a DOF of approximately 2 μm is observed with the DOF dropping approximately linearly to 0.8 μm at a CD of 70 nm.

Another crucial image parameter is line-edge roughness (LER). One can also find the LER-limited DOF by repeating the process window analysis while setting constraints on the LER instead of the CD. Doing so with a LER threshold of 10% of nominal CD yields the second set of bars shown in the Fig. 4 plot. The LER is defined as the 3σ single-sided line-edge deviation from a straight line. 10% relative LER constraints are seen to limit the minimum resolution to 80 nm.

The results presented above are based on dark field prints minimizing the effect of flare. Noting that the intrinsic flare in the set-2 optic used here is approximately 20%,[15] one would expect significant performance degradation for bright field imaging. Figure 5 shows bright field DOF results using the same analysis criteria used in Fig. 4. In terms of the CD-limited process window, the flare-induced contrast loss causes a DOF loss of approximately 25%. Considering the LER-limited process window, however, we see nearly 50% DOF reduction at the larger CDs and no 10% EL DOF whatsoever for 80 and 70 nm half pitch features.

As previously demonstrated,[8] nominal exposure offset can be used to dramatically improve the minimum printable semi-isolated feature size. For example, Fig. 6 shows 37 nm lines on 240 nm pitch as achieved by an approximate 35%

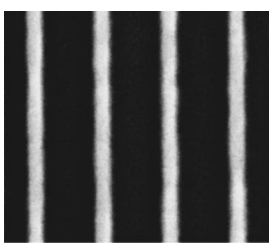

FIG. 6. Resist image of 37 nm lines on 240 nm pitch printed by setting the exposure level to approximately 35% over nominal for 80 nm coded features.

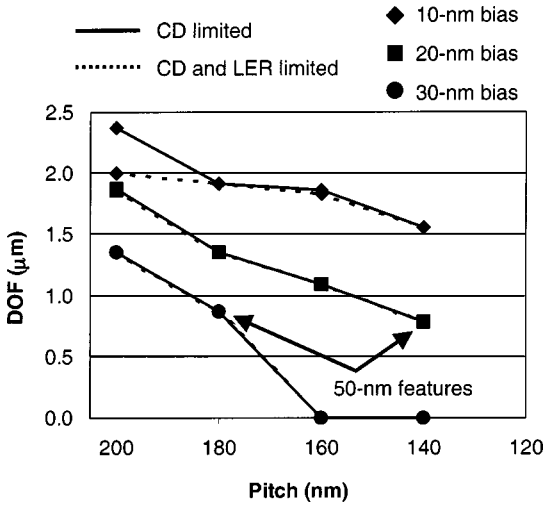

FIG. 7. DOF as a function of pitch for various bias values, where the bias corresponds to the exposure-induced feature shrink in nm relative to the coded half pitch. For example, for 50 nm features, which can be achieved with 20 nm bias on 140 nm pitch or 30 nm bias on 180 nm pitch, yield DOFs of 0.8 and 0.9 μm, respectively.

overdose of 80 nm coded lines. In addition to reducing the CD, the LER is also improved. It is also important to consider the process window performance in this offset exposure method. Figure 7 shows the DOF as a function of pitch for various bias values, where the bias corresponds to the exposure-induced feature shrink in nm relative to the coded half pitch. Considering, for example, 50 nm features, these can be achieved with 20 nm bias on 140 nm pitch or 30 nm bias on 160 nm pitch. These cases yield a DOF of 0.8 and 0.9 μm, respectively, roughly equivalent to the 70 nm feature DOF without bias. It is also interesting to note that up to 20 nm bias can be achieved without loss of DOF as a function of half pitch and that the DOF is actually improved as seen in the 10 nm bias case. Moreover, the bias causes the CD and LER limited process windows to converge.

IV. SUMMARY

The static microfield exposure station installed at Lawrence Berkeley National Laboratory's Advanced Light Source synchrotron radiation facility has been used to lithographically characterize the set-2 optic, which is now integrated into the ETS. These results serve both as a source for valuable EUV learning and provide a performance benchmark for operation of the ETS with the set-2 optic. Process-window results on equal line/space features show approximately a 2 μm DOF when operating at a k_1 factor of 0.75 (100 nm CD) and nearly 1 μm DOF at 70 nm CD. On semi-isolated features, approximately 1.5 and 1 μm DOF is achieved for 60 and 50 nm features, respectively.

In addition to the results presented here, process window results have also been characterized for isolated line features and contacts.[16] On isolated features, better than 2 μm DOF was achieved all the way down to 70 nm CD. Also, printing of 70 nm contacts on 270 nm pitch was demonstrated to support a DOF of nearly 0.5 μm.

ACKNOWLEDGMENTS

The authors are greatly indebted to Kevin Bradley, Rene Delano, Paul Denham, Brian Hoef, Gideon Jones, Seno Rekawa, Ron Tackaberry, and Eugene Veklerov for expert engineering and fabrication support, and to the entire CXRO staff for enabling this research. This research was supported by the Extreme Ultraviolet Limited Liability Company and carried out at Lawrence Berkeley National Laboratory under the auspices of the DOE Office of Basic Energy Science.

[1]R. Stulen and D. Sweeney, IEEE J. Quantum Electron. **35**, 694 (1999).
[2]H. Meiling, J. Benschop, R. Hartman, P. Kürz, P. Høghøj, R. Geyl, and N. Harned, Proc. SPIE **4688**, 1 (2002).
[3]D. Attwood, G. Sommargren, R. Beguiristain, K. Nguyen, J. Bokor, N. Ceglio, K. Jackson, M. Koike, and J. Underwood, Appl. Opt. **32**, 7022 (1993).
[4]H. Medecki, E. Tejnil, K. A. Goldberg, and J. Bokor, Opt. Lett. **21**, 1526 (1996).
[5]K. A. Goldberg, P. Naulleau, P. Batson, P. Denham, H. Chapman, and J. Bokor, J. Vac. Sci. Technol. B **18**, 2911 (2000).
[6]J. Goldsmith *et al.*, Proc. SPIE **3676**, 264 (1999).
[7]K. Hamamoto, T. Watanabe, H. Tsubakino, H. Kinoshita, T. Shoki, and M. Hosoya, J. Photopolym. Sci. Technol. **14**, 567 (2001).
[8]P. Naulleau *et al.*, J. Vac. Sci. Technol. B **20**, 2829 (2002).
[9]P. Naulleau, K. Goldberg, P. Batson, J. Bokor, P. Denham, and S. Rekawa, Appl. Opt. **42**, 820 (2003).
[10]P. Naulleau *et al.*, Proc. SPIE **4688**, 64 (2002).
[11]D. W. Sweeney, R. Hudyma, H. N. Chapman, and D. Shafer, Proc. SPIE **3331**, 2 (1998).
[12]K. Goldberg, P. Naulleau, J. Bokor, and H. Chapman, Proc. SPIE **4688**, 329 (2002).
[13]D. O'Connell *et al.*, Proc. SPIE (to be published).
[14]S. Lee, D. Tichenor, and P. Naulleau, J. Vac. Sci. Technol. B **20**, 2849 (2002).
[15]S. Lee *et al.*, Proc. SPIE **4688**, 266 (2002).
[16]P. Naulleau *et al.*, Proc. SPIE (to be published).